CRYSTAL GROWTH TECHNIQUES FOR PEROVSKITE PHOTOVOLTAIC APPLICATIONS

Abstract

Silicon based conventional solar cells have dominated the photovoltaic (PV) market as they have high efficiency even though their production cost is comparatively high. Continuous efforts for an alternative to the conventional cells have been made across the globe to reduce the cost. One of the most standout in the search of an alternative is the hybrid solar cells – a blend of both organic and inorganic materials. Organic materials are keenly priced, easy to process and their functionality can be altered by chemical synthesis and molecular engineering. Inorganic semiconductors have high absorption coefficients, by possibility of varying size of nanoparticles the absorption range can be tailored with tunability of band gap. Hybrid halide perovskites possess quite interesting properties such as large absorption coefficients, high carrier mobility, long carrier life time, long carrier diffusion length and a tunable energy band gap. These properties have attracted more attention for optoelectronic applications, especially in photovoltaic devices. The evolution of perovskite solar cells (PSCs) towards a formidable performance would depend on its synthesis techniques. In this book chapter, we present the various methods used in the synthesis of single crystals of hybrid perovskites and address the main synthesis issues pertaining to PSCs.

Keywords: Perovskite solar cells, Hybrid solar cells, Tolerance factor, Absorption coefficient, Gamma-butyrolactone.

Authors

Ajay Kumar
Department of Electronic Science
University of Delhi, South Campus
New Delhi, India.

Ashish
Department of Physics
Central University of Rajasthan
Ajmer, India.

Sanjeev Kumar
Department of Physics
Motilal Nehru College, South Campus
New Delhi, India.

Udaibir Singh
Department of Electronics
Acharya Narendra Dev College
University of Delhi
New Delhi, India.

Naorem Santakrus Singh
Department of Physics
Hindu College, University of Delhi
Delhi, India.
santakrus@hinducollege.ac.in

I. INTRODUCTION

Amongst the many renewable sources of energy - hydro, wind, solar, etc., solar energy stand out as the most important energy source and in fact all the renewable energy sources depend on it directly or indirectly. The earth receives 2.9×10^{15}kW of energy every day from the sun in the manner of electromagnetic radiations which is around 100 times the total energy consumption of the entire globe annually [1]. An affirmative use of this energy could afford the ever increasing global energy demand and provide an alternative to the depleting fossil fuels in a sustainable way without leaving any significant impact on the environment. In light of recent economic and scientific advancements as well as the seeking global warming remedies, photovoltaics now holds great promise as a potential alternative to nuclear and fossil fuels. Albeit the PV industry is predominantly occupied by silicon photovoltaic devices, the innovations in fabrication protocols [2-3], chemical compositions [4] and relevant phase-stabilizations [5-7] has given the PSCs the potential to challenge the well-established Si PV market. With the emergence of metal halide perovskite solar cells as a promising research field, PSC efficiencies have significantly increased, rising from 3.8% in 2009 [8] to 23.7% in 2018. These improvements in efficiency put them on level with cutting-edge developments in thin-film solar cell technologies like copper indium gallium diselenide (CIGS) and CdTe [9-10]. The thermodynamic limit of the band gap has been reached by perovskite solar cells, which have a substantiated verified power conversion efficiency of 25.2%, or 80.5% [11-12]. The theoretical limit for silicon solar cells is 80.9%, thus this accomplishment is comparable. Efficiency of various kinds of solar cells as reported in nrel website [13] is shown in Fig. 1.

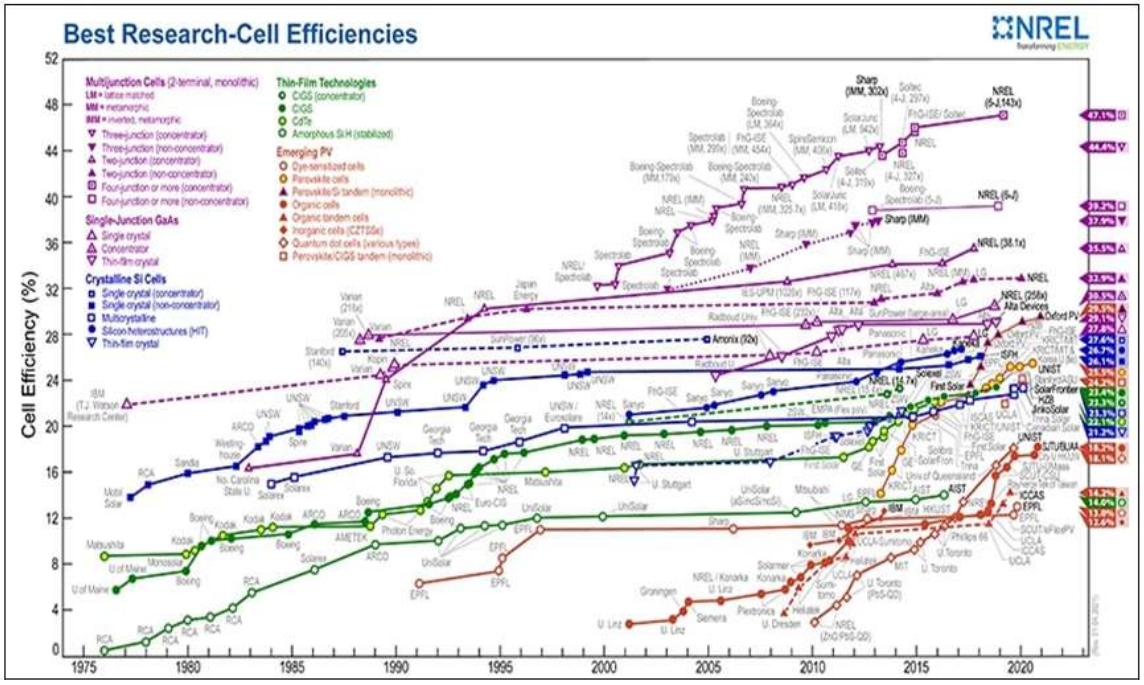

Figure 1: Efficiency of Various types of Research Solar Cells.

This tremendous development is made possible by the tunable properties of the perovskites designed through various synthesis techniques. In this chapter, we present the various methods used in the synthesis of single crystals of hybrid perovskites focusing

mainly on three methods giving a deep insight into all readily available protocols for crystal growth and the most method to obtain high quality single crystals. A sketch of the possible future roadmap is also included to address the main synthesis issues pertaining to PSCs. The manuscript has been arranged in the following manner: (I) Introduction (II) Perovskite structure (III) Performance characteristics of a solar cell (IV) Perovskite tolerance factor (V) Synthesis process (primary solvent and methods) and (VI) Conclusion.

II. PEROVSKITE STRUCTURE

In the current scenario, hybrid organic-inorganic perovskites are receiving a lot of attention, especially the ABX_3 configured organometal halide perovskites. These materials have a ton of promise for use in the photovoltaic industry [14]. In this structure, "A" indicate a more substantial organic cation, such as formamidinium $(CH(NH_2)_2)^+$ or FA) or methylammonium ($CH_3NH_3^+$ or MA). Ni^{2+}, Co^{2+}, Fe^{2+}, Cu^{2+}, Ge^{2+}, Sn^{2+}, Pb^2 and Mn^{2+} are examples of smaller divalent metal cations, while 'X' indicate for a monovalent halide anion like F^-, Cl^-, Br^-,I^- and so on. A, B, and X are arranged in the unit cell layout with 'A' occupying the corners, 'B' in the body centre, and 'X' at the centre of the faces as shown in Fig. 2.

When compared to other hybrid perovskites, lead-organic iodide perovskites have shown to have more useful characteristics. Noteworthy perovskite compositions encompass methylammonium lead iodide ($CH_3NH_3PbI_3$ or $MAPbI_3$), methylammonium lead chloride ($CH_3NH_3PbCl_3$ or $MAPbCl_3$), formamidinium lead iodide ($CH(NH_2)_2PbI_3$ or $FAPbI_3$), and variations involving methylammonium tri-iodide mixed with chloride, like chloride-doped $MAPbI_3$ ($CH_3NH_3PbI_{3-x}Cl_x$), among others. These substances exhibit minor electrical, photovoltaic, ferroelastic, ferroelectric and pyroelectric capabilities. The tetragonal phase of $MAPbI_3$ is a good example of this. $MAPbX_3$, the substitution of X = Cl^-, Br^-, I^- correspond to narrow the band gap as 3.11eV, 2.35eV, and 1.6eV respectively.

Replacement of small MA (1.8Å) with larger FA (1.9-2.2Å) forming $FAPbI_3$, the band gap reduced from 1.6eV to 1.48eV [15]. The cubic phase, which exists at high temperatures (T_C> 327.4K), and the tetragonal phase, which exists at room temperature, are the prominent phases that have been observed in $MAPbI_3$. The space groups Pm3m and I4/mcm, which define an ideal cubic symmetrical structure with a volume of 247.1 and lattice parameters a = b = c = 6.276, are what distinguish the crystallographic structures of $MAPbI_3$ [16].

Similar to this, two distinct phases of $FAPbI_3$, also known as $[HC(NH_2)_2]PbI_3$, can be identified at 298 K: a cubic-perovskite black phase (alpha-phase) and a non-perovskite yellow phase (delta-phase) with a hexagonal structure. At normal temperature, the cubic-perovskite black phase of $FAPbI_3$ contains the Pm3m space group, which is similar to the structure of MAPbI3 at high temperatures (T > 327.4K).The cell volume and lattice parameter, in this case, were determined to be 6.362Å and 257.5$Å^3$, respectively [16].

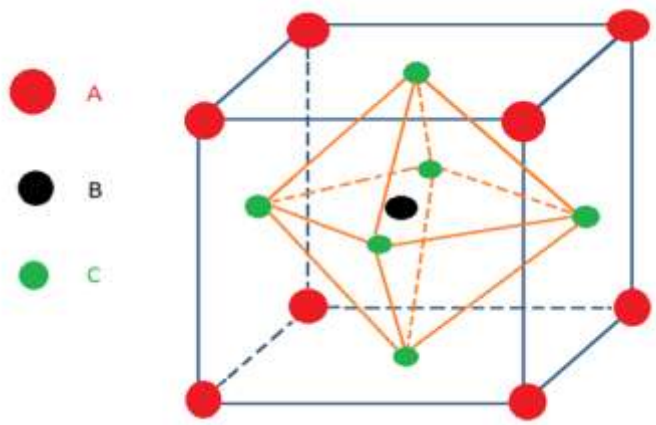

Figure 2: Basic Structure of Perovskites with ABX_3 Formula.

The properties and application of some significant perovskite materials are display in Table 1 [16-18]. For the purpose of making capacitors, $CaTiO_3$'s dielectric property is exploited and $BaTiO_3$ is used in capacitor and sensor. The piezoelectric property of $PbTiO_3$ and $LiNbO_3$ is used in pyro-detector. Good absorption property of $MAPbI_3$ and $FAPbI_3$ is used in solar cells and photodetector application.

Table 1: Properties and Applications of Some perovskite Materials

S.No.	Materials	Properties	Applications
1.	$CaTiO_3$	Dielectric	Capacitor
2.	$BaTiO_3$	Dielectric	Capacitor, Sensor
3.	$PbTiO_3$	Piezoelectric, Pyroelectric	Acoustic transducer, Pyrodetector
4.	$LiNbO_3$	Piezoelectric	Pyrodetector, Surface acoustic wave
5.	$MAPbI_3$	Strong absorption coefficient, high mobility	Solar cells, Photodetectors
6.	$FAPbI_3$	Strong absorption coefficient, long carrier life time, high mobility	Solar cells, Photodetectors

III. PERFORMANCE CHARACTERISTICS OF A SOLAR CELL

In dark as well as illuminated environments, a solar cell's I-V curves are exhibited in Fig.3. The forward bias voltage does not surpass the voltage of open circuit in the absence of light until there is a small current present. Two particular possibilities appear when exposed to illumination:

The solar cell has zero voltage across it in the (a) short circuit current (I_{sc}) condition, which corresponds to the maximum photocurrent flow.(b) Open circuit voltage (V_{oc}) state: The photocurrent has equilibrated to zero in this condition, which denotes the maximal

voltage that can be obtained from a solar cell.The multiplication of voltage and current peaks at the point of maximum power (P_m) ($I_m x V_m = P_m$).

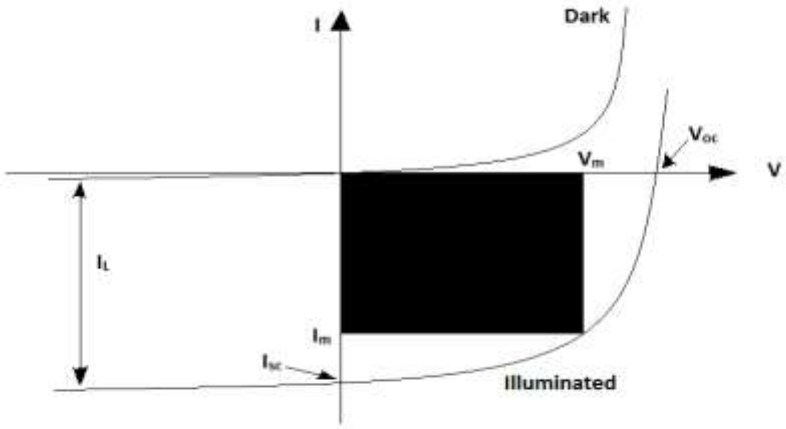

Figure 3: I-V Characteristic of Solar Cell (Dark and Illuminated)

The I_{sc} and V_{oc} of the solar cell are found at the intersection of the horizontal and vertical axes. Peak power ($I_m x V_m = P_m$) is indicated by the shaded zone and occurs at the intersection where voltage and current multiply to their maximum value.
The power conversion efficiency (PCE) of solar cell is expressed as follows:

$$\text{PCE } (\eta) = \frac{(V_{oc} x I_{sc} x FF)}{P_{in}} \quad (1)$$

And the fill factor is defined as

$$\text{FF} = \frac{(I_m \times V_m)}{(V_{oc} \times I_{sc})} \quad (2)$$

Where I_{sc} represents the short circuit current, V_{oc} is the open circuit voltage, FF is the fill factor and P_{in} denotes the incident input power. Standard reference spectra allow a valid comparison of device performance of photovoltaic devices from different sources, the international standardized incident spectrum of AM1.5 at 1000 W/m^2 intensity is used. AM is the air mass defined as 1/cosφ, where φ is the angle formed by the vertical and the sun's position. Air mass 1.5 (AM1.5), correspond to φ = 48°. The maximum intensity of sun light occurs when the sun is straight overhead i.e., AM1.0 at φ = 0°. Air mass zero (AM0) correspond to the solar spectrum measured beyond Earth's atmosphere. AM0 is useful for space and satellite applications, whereas AM1.5 is useful for terrestrial solar cell application [19-21].

IV. PEROVSKITE TOLERENCE FACTOR

Victor Moritz Goldschmidt's tolerance factor (t) helps to explain how the ABX_3perovskite structure deforms and maintains stability. According to this definition:

$$t = \frac{(r_A + r_x)}{\sqrt{2}(r_B + r_x)} \quad (3)$$

Where r_A, r_B, and r_x represent the corresponding ionic radii of A, B, and X components of perovskite structure [22]. The value of t can be used as a factor to determine if the solution of ions can create a formable perovskite structure or not. Table 2, describe the crystal structure along with their size description of cation and anion on the position of A, B and X corresponding to different range-value of tolerance factor [23-25].

Table 2: Tolerance Factor (*T*) and Possible Structure of Perovskite.

S.No.	Tolerance factor (t)	Description	Structure
1.	$t > 1$	A is large than B	Hexagonal or Tetragonal
2.	$t = 1$	A are B are ideally equal	Ideally cubic
3.	$0.9 \leq t \leq 1$	A and B are ideal structure	Cubic
4.	$0.7 \leq t \leq 0.9$	A is small or B large	Orthorhombic/ rhombohedral
5.	$t < 0.7$	A and B have similar radii	Dissimilar structure

When the value of *t* is from 0.9-1, the ideal cubic crystal structure of perovskite is generally formed. Accordingly, when the value range of *t* is 0.7-0.9, A is small or B larger, the possible crystal structure is tetragonal and orthorhombic or rhombohedral, while the value of t is larger than 1, A is large than B, the possible crystal structure is either hexagonal or tetragonal. Therefore, when the tolerance factor value ranges from 0.7 to 1.0, a stable crystal structure of perovskite exist. Non-perovskite structure is formed when $t < 0.7$ and $t > 1.0$.An schematic representation of various perovskite materials as per their tolerance factor (t = 0.7 - 1.0) is depicted in Fig. 4 [26].

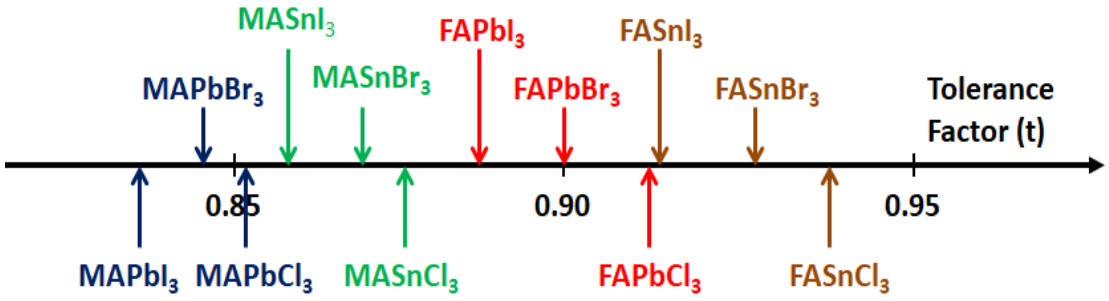

Figure 4: Tolerance Factors (T) of a Series of Organic-Inorganic Perovskites

Another criterion for a new tolerance factor (τ) suggested by C. J. Bartel [27] has the formula

$$\tau = \frac{r_x}{r_B} - n_A\left(n_A - \frac{r_A/r_B}{ln(r_A/r_B)}\right) \quad (4)$$

Where r_A, r_B, and r_x, represent their corresponding ionic radii of A, B, and X components of perovskite structure, and n_A is the oxidation state of A, $r_A > r_B$ and $\tau < 4.18$ indicates perovskite. With this new criterion, from the experimental data set of 576 ABX_3 materials where ($X = O^{2-}$, F^-, Cl^-, Br^-, I^-), 92% compounds were identified as perovskite or non-perovskite. In another set of data, 91% compounds out of 918 were also correctly

distinguished between perovskite and non-perovskite. However, the use of Goldschmidt tolerance factor (*t*), could correctly differentiate hardly 74% of the materials between perovskite and non-perovskites. As per the study reported in by C. J. Bartel et al [27], a stable perovskite would be formed when *t* lies in the range of 0.825 - 1.059.

V. SYNTHESIS PROCESS

It consists of two important components: (i) primary solvent (required for dissolving the precursor completely to follow reaction) and (ii) synthesis methods (significant forcrystal growth)

1. **Primary Solvent:** Organic-inorganic hybrid perovskite materials require a solvent for formation of thin film and single crystal by the method of solution growth technique. Polar aprotic solvents (solvent that has no O-H or N-H bond, but hold C=O or S=O bond), such as di-methylformamide (DMF), dimethylsulfoxide (DMSO), N-methyl-2-pyrrolidone (NMP), and gamma-butyrolactone (GBL) are essential for precursor solution. So, its polar aprotic nature is the requisite characteristics for the solvent, which can dissolve perovskite precursors, otherwise the device morphology gets distorted. A summary of various properties of different solvents is presented in Table 3 [28, 29].

Table 3: Comparison between Different Solvents.

S.No.	Solvent	Boiling point (^oC)	Vapor pressure at room temp. (Torr)	Dielectric constant	Viscosity (cP)	Chemical formula
1	DMF	152	1.5	36.7	0.92	C_3H_7NO
2	DMSO	189	2.7	46.7	2.00	C_2H_6OS
3	NMP	202	0.3	33.0	1.65	C_5H_9NO
4	GBL	204	0.375	39.1	1.90	$C_4H_6O_2$

Boiling point and vapor pressure of solvent is an important factor for crystallization and thin film formation. Both must recorded during the crystallization route, that is, fast or slow. Rapid crystallization is encouraged by an increased vapor pressure since it lowers the boiling point and increases volatility. On the other hand, a greater boiling point raises the temperature and length of time needed for crystallization [28, 29]**.** In general, GBL is an appropriate solvent for I-based perovskite, while DMF is suitable for Br-based perovskites. When assessing crystal quality, choosing the right solvent has always been important. Solvents including DMF, DMSO, and GBL are frequently used with hybrid perovskites. The solubility of MAX and PbX_2 (where X = Cl, Br, I) precursors in these given solvents are quite significant accordingly. It has been noted that $MAPbI_3$crystallizes more aptly from GBL while $MAPbBr_3$ crystallizes better from DMF and in the same pattern, the solvents for $FAPbX_3$ (where X = Cl, Br, I) can be made [15, 30].

2. **Growth of Single Crystal by Different Methods:** A lot of processes are described in literature for growth of single crystals of organic-inorganic halide based perovskite material. These methods include: Bridgman growth method [31-33], Droplet-pinned crystallization method [34], Solvo-thermal growth method [35, 36], Solution temperature

lowering method [37, 38], Anti-solvent vapor-assisted crystallization method [39-41], Layered solution growth method [42], Slow evaporation method [43, 44], Inverse temperature crystallization [45-53] and Modified inverse temperature crystallization [54-62]. Each of these techniques has its own characteristics as well as advantages and disadvantages which are described in detail in the given references. Based on the ease to grow organic-inorganic and hybrid large size single crystal perovskites, whose size lies in range 1mm - 20mm, under ambient conditions, three methods are more prominent which namely: slow evaporation method, Inverse temperature crystallization method and Modified inverse temperature crystallization. These methods broadly discussed below. The crystals so synthesized have several useful property i.e trap density, carrier lifetime, carrier mobility, optimum and gap, and optoelectronic application like photodetector and solar cell havinggood efficiency at low cost [29].

3. **Slow Evaporation Method (SE):** One of the simplest and traditional methods for growing single crystals is SE [8, 23, 43, 44] and is suitable for air stable samples (compounds which are not sensitive to moisture or air). This process used for growing both organic and inorganic sample in majority of single crystals, In this method, a saturated or nearly saturated clear solution is get ready by blending together two or more reactant for suitable solvent. Clear solution is then shifted in a vial or crystal growing dish which is covered with perforated cap or aluminium foil having small holes. A schematic representation of this method is shown in Fig. 5.

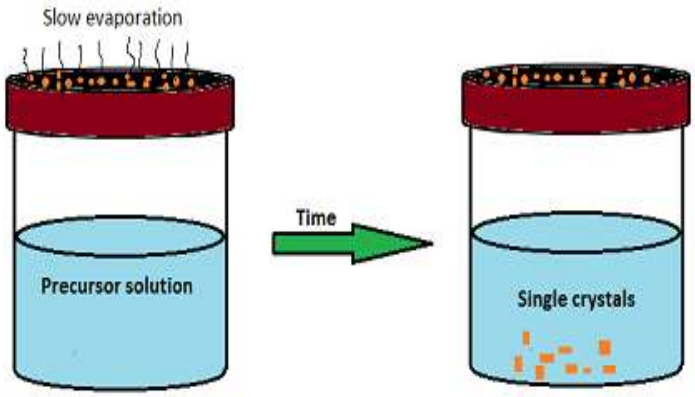

Figure 5: Schematic Representation of Synthesis of Single Crystal by SE Method

Synthesis of perovskite crystals by slow evaporation are investigated by Xionget. al. [43] and Daub ET. al. [44]. Dissolving a mixture of $BACl_2$ and PbI_2 in conc. HCl aqueous sol. results in the formation of small crystals of BA_2PbX_4 (BA = benzylammonium and X = Cl, Br, I) whereas the use of DMF solution instead of conc. HCl at 90^0C produced large size transparent crystals via slow evaporation.

A mixture of 0.20g $Pb(SCN)_2$ and 0.15g MAI was dissolved in 0.6 mL of DMF solution is stirred at 60^oC temperature to get a clear solution. Afterwards, subjected to gradual evaporation under normal room temperature, a black colored single crystal of $MA_2Pb(SCN)_2I_2$ was obtained in which I^- was partially substituted by SCN^- ion [44]. Formation of high-quality perovskite single crystals from liquids with low boiling points up to 100^0C, the slow evaporation method is quite successful. The use of this approach

for prepration of perovskite single crystal has been restricted by the less solubilities of the reactants of the perovskite precursor. So this method emergesas challenging to control precisely that resolutely limit its applications.

4. **Inversion Temperature Crystallization Method (ITC):** ITC method is appropriate for the materials in which solutes have the tendency of higher degree of solubility at high temperature. In this, more precursors will be dissolved in the solvent for crystallization when heated. Furthermore, solubility of solute in solvent decreases with increases in temperature. This allows a retrograde solubility or inverse temperature method to grow single crystal [15, 45]. Currently, ITC method is widely used to grow organic-inorganic hybrid perovskite large size single crystal with facile and rapid route [46]. A schematic diagram of ITC method is displayed in Fig. 6.

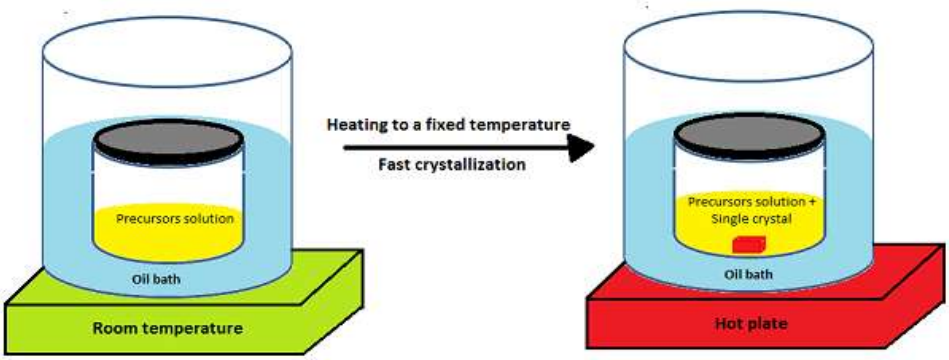

Figure 6: Schematic Representation of the Inverse Temperature Crystallization (ITC) Method

First adopted by M. I. Saidaminov, the ITC method has successfully synthesized many organic-inorganic perovskite crystals of $MAPbI_3$, $MAPbBr_3$, $MAPbCl_3$, and FAPbI3 [30]. A vital feature of this technique is that resultant crystals are of good quality, shape controlled and minimum time consuming. Precipitates of $MAPbBr_3$ are formed in concentrated solution of DMF at high temperature and fail to precipitate in other solutions such as DMSO and GBL. Similarly, $MAPbI_3$ crystallizes only in GBL, exhibiting solvent specific characteristic for crystal growth of perovskites. The growth rate of $MAPbI_3$ crystal was calculated to be $3mm^3h^{-1}$ for initial hour and increases to $9\ mm^3h^{-1}$ for the second hour and $20mm^3h^{-1}$ for next following hour. In case of $MAPbBr_3$ crystals, faster growth rate was observed reaching up to $38mm^3h^{-1}$ in the third hour. Tauc plots estimates the band gap for $MAPbBr_3$ and $MAPbI_3$ single crystal to be 2.18 eV and 1.51 eV corresponding to the photoluminescence peaks at 574nm and 820nm respectively. Trap density and carrier mobilities for $MAPbBr_3$ crystals calculated to be 3 x $10^{10}cm^{-3}$ and 24.0 cm^2V^{-1} s^{-1}.Similarly, for $MAPbI_3$ crystals, the calculated trap densities and carrier mobilities were 67.2 cm^2V^{-1} s^{-1} and 1.4 x $10^{10}cm^{-3}$. Carrier diffusion length [$L_D = (\mu\tau k_BT/e)^{1/2}$ (where T is temp., τ is carrier lifetime with μ is mobility)] were obtained for a best case using longer carrier lifetime ~4.3µm and ~10.0µm and for worst case using shorter carrier lifetime ~1.3µm and ~1.8µm for $MAPbBr_3$ and $MAPbI_3$ respectively [30]. A transparent and colorless parallelepiped shape single crystal of $MAPbCl_3$, having a typical dimension of 2×4×4 mm^3, was synthesized by G. Maculan et.

al [47] by ITC method using two precursors of MACl and $PbCl_2$ in acomposition of DMSO and DMF (1:1 v/v) solvent. Optical properties of $MAPbCl_3$ crystal exhibit PL peak at 440nm and sharp absorption edge at 435nm. Lattice constant of the crystal was determined to be a = 5.67 Å as per the powder X-ray diffraction (PXRD) and the valence band maxima (VBM) $MAPbCl_3$was estimated to be -5.82eV through photoelectron spectroscopy in air (PESA) measurement. The carrier dynamics components for both slow ($\tau \sim 662$ ns) and fasts ($\tau \sim 83$ ns) were observed by transient absorption (TA). Slow and fast components are probably associated with bulk and surface of crystal. At low electric field, electrical conductivity (σ) was found to be 2.7 x 10^{-8} $\Omega^{-1}cm^{-1}$ and trap density to be ~3.1 x $10^{10}cm^{-3}$ and diffusion length were obtained for a best case using longer carrier lifetime ~8.5µm and for worst case using shorter carrier lifetime ~3.0µm $MAPbCl_3$. Responsivity ($R = (I_{light} - I_{dark}) / P_{light}$) and Detectivity ($D = R / (2qJ_{dark})^{1/2}$) were calculated as 46.9 mA/W and 1.2 x 10^{10} [47]. Another perovskite single crystal synthesized by ITC is $CH_3NH_3PbI_3$ ($MAPbI_3$) from two precursors CH_3NH_3I and PbI_2dissolved in GBL stir vigorously at 100°C in the molar ratio of 1:1 in ambient conditions in a nitrogen globe box [48]. Temperature of solution rapidly increasesfrom 100°C to 190°C and after 25 minutes, a black colored crystal of $MAPbI_3$having rhombic dodecahedral or rhombo-hexagonal dodecahedral structure having space group I4/mcm was obtained. However, the crystal gets dissolved again when the solution cools down to room temperature shown in Fig. 7.

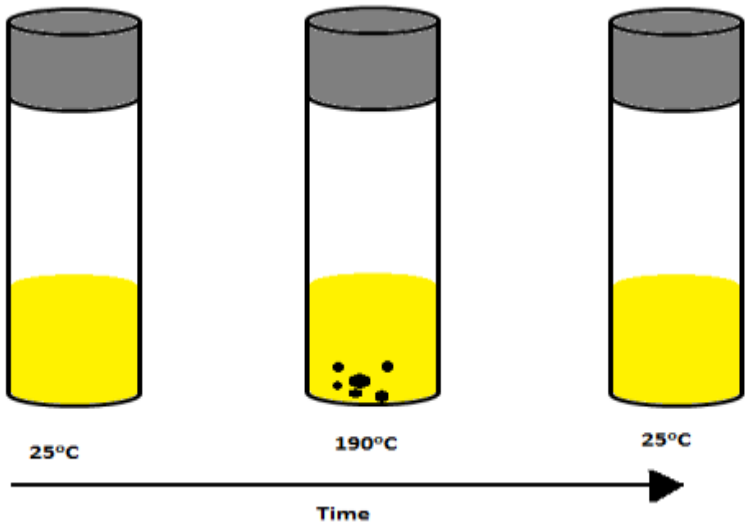

Figure 7: Schematic Experimental Observation of $CH_3NH_3PbI_3$ ($Mapbi_3$) Crystal Growth at High Temperature while the Crystals Disappear at Decreasing Temperature.

Photoluminescence (PL) and cathodoluminescence (CL) spectra of $CH_3NH_3PbI_3$ were observed to have single emission peak at 775 nm after excitation at 480nm in PL spectra. PL and CL peaks are almost the same and lies within the expected range for the band gap around 1.5eV of tetragonal $CH_3NH_3PbI_3$ [26, 48]. ITC method is superior for growing large size and high quality single crystal of $CsPbBr_3$ under ambient conditions [49]. Two precursors namely CsBr and $PbBr_2$ with molar ratio 1:2 dissolved in DMSO solvent followed by the addition of DMF and cyclohexanol (CyOH) when heated at 90°C, results in the formation of 1-3 nuclei. A continuous heating of the solution at 110°C for 12 h lead to the growth of an orange-colored, flat and appoximately 8 mm long $CsPbBr_3$

single crystals. Use of DMF and cyclohexanol (CyOH) mixture in the reaction prevents the unwanted formation of polycrystals or multinuclei crystals surface [49].

Formation of a high-quality lead iodide single crystal of $FA_{1-x}Cs_xPbI_3$ (x = 0 and 0.1) with mix cation via ITC method is reported in S. Kawachi et al [50] and investigated its crystal structure and thermodynamic properties. Firstly, precursors FAI, PbI_2 and CsI were dissolved in GBL solvent and stired for ~1h at room temp. and then the solution was heated (i) at 115^{o}C for x = 0 and (ii) at 120^{o}C for x = 0.1. On heating the solution for 40-60 minutes, single crystals of $1-2mm^3$ with hexagonal pyramidal shape were obtained. Highly stable perovskite single crystals having mixed cation and halide compositions $(FAPbI_3)_{0.9}(MAPbBr_3)_{0.05}(CsPbBr_3)_{0.05}$ with band gaps of $1.52eV$ was reported by L. Chen [51]. The crystal showed good stability against water and oxygen for 10000 h and 1000 h respectively with magnificent thermal stability. The result showed high power conversion efficiency for long term stable provskite solar cells application. M. Pratheek et. al. [52] reported the synthesis of large $MAPbI_3$ perovskite single crystals using simplified ITC method at room temperature, without glove box or inert atmosphere. Single crystals of size $12mm$ having remarkably high environmental stability were developed in open atmosphere. XRD results confirm the non-degradation of the material for a month. However, more studies are required to explore this feature of single crystal with long term air stability. Y. Liu et al [53] prepared a triple-cation mixed-halide (TCMH) $FA_{0.85}MA_{0.1}Cs_{0.05}PbI_{2.55}Br_{0.45}$ (FAMACs) single crystals by ITC method in organic solution. Precisely, the stoichiometric molar ratio of precursors FAI, MABr, CsBr, $PbBr_2$, PbI_2 were dissolved in GBL solvent to prepare 1.3M concentration of the solution. After complete dissolution of precursors into the solvent, 2% (in volume) of formic acid was mixed into the solution and stirred and the solution filtered by 0.8µm pore size PTFE filter paper. Filtered solution was placed into the oven for 5 h at temperature 60°C. Then, the temperature increased up to 110°C with steady rate of 5°C per day that lead to the formation of small size crystals in the crystallizing dish. To obtain inch size FAMACs single crystals, well-shaped crystals from the solution were transferred to the freshly prepared solution which was already heated at 90^{o}C.The size of added crystal grows gradually as the temperature was increased to 110^{o}C, and finally inch-sized triple-cation mixed-halide (TCMH) $FA_{0.85}MA_{0.1}Cs_{0.05}PbI_{2.55}Br_{0.45}$ (FAMACs) single crystals were obtained. XRD and high resolution (HRXRD) were done by using 2700BH X-ray diffractometer and X'Pert pro MRD respectively. Thermal analysis (TGA), UV-Vis-NIR absorbance spectra and Space-charge-limited current (SCLC) measurement also measured.

5. **Modified Inversion Temperature Crystallization Method (MITC):** The MITC method is employed to cultivate a single crystal of substantial size of perovskite by using a seed crystal. The method involves two directions for growing large size single crystal as outlined here: (1) Seed crystal growth for hybrid organic-inorganic perovskite materials and (2) Impurity avoidance of undesired materials for all inorganic perovskite materials [13, 16].

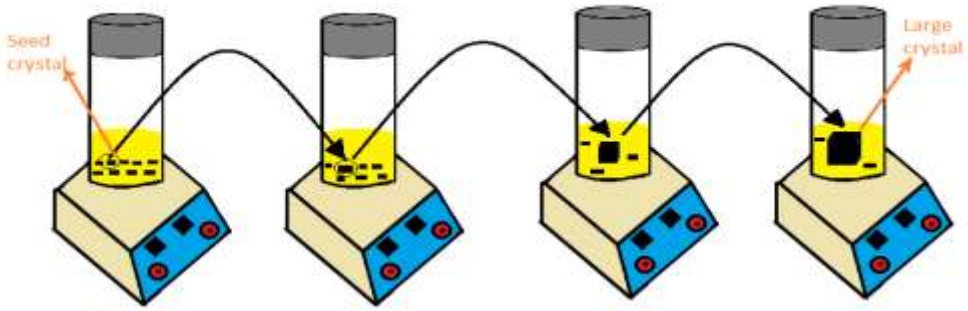

Figure 8: Schematic Representation of MITC Method using Seed Crystal for the Growth of Large Sized Single Crystal.

Y. Liu et. al. [54, 55] has grown various large size organic-inorganic perovskite crystals of $MAPbI_3$ and $FAPbI_3$ using MITC method. They also studied its various parameters i.e diffusion length, trap density, carrier lifetime, and carrier mobility. A step by step pictorial representation for growing large size and good quality single crystals of $MAPbX_3$ (where X = Cl^-, Br^-, I^-) and $FAPbI_3$ is displayed in Fig 8. Firstly, FAX or MAX and PbX_2 needs to be dissolved in appropriate solvent such as GBL, DMF and DMSO then stirred overnight at high temperature; precursors lose their solubility resulting in seeding of a many small crystals having size about $1-2mm$. A good quality crystal seed needs to be chosen which is placed into a freshly prepared precursor solution. A further heating of the solution overnight at 100^oC would result in the gradual formation of large size crystal. A repetition of the process multiple times would produce much larger crystals. The crystals so produced had a low trap density signified by the blue shift in photoluminescence spectra and these spectra shifts toward red when compared with corresponding thin film. A wafer of $FAPbBr_3$ crystal shows a photoresponse almost 90 times higher than its corresponding thin film. Results of differential scanning calorimetry (DSC) and thermo-gravimetric analysis (TGA) indicates a higher stability of $MAPbI_3$ crystals at high temperature as compared to $MAPbI_3$ thin films. The single crystals of $MAPbCl_3$ was cuboidal shape and transparent and $MAPbBr_3$ was cuboidal shape and orange in color where as $MAPbI_3$ crystals are generally dodecahedrons in shape but sometimes rhombohexagonal dodecahedrons [26]. Large size crystals of $MAPbI_3$ obtained via MITC method [56] was found to have several interesting properties such as non-linear optical properties and amplified spontaneous emission (ASE) which may be quite useful for laser applications [57]. Measurement of non-linear optical properties by open aperture Z-scan technique confirms a lower absorption coefficient than that of $MAPbBr_3$single crystal [58] and polycrystalline$MAPbI_3$ [59]. Q. Han et al. [18] reported a crystal of $FAPbI_3$ grown by MITC method and investigated structural, electrical and optical properties of the crystal. Photoluminescence results show a red shift emission with lower band gap value of these crystals with larger value of carrier mobility and carrier lifetime.

H. S. Rao et al [60] A $16\mu m$ thick laminar single crystal of $MAPbBr_3$ was prepared by MITC method having high mobility, high power efficiency, good crystal quality and low trap density than the thin film. First, using TiO_2 coated FTO glass, a box with an appropriate space gap was built for a laminar, controlled thickness single crystal

of $MAPbBr_3$. Precursors of $PbBr_2$ and $MABr$ in DMF solution were inserted and the solution was heated at 90°C with homothermalaluminum block Y. Rakita et.al. [61] Employed saturated precursors of CsBr and $PbBr_2$ in DMF solution in order to grow $CsPbBr_3$ crystals. In a hit and trial process, they tried nine antisolvents, out of which three antisolvents - acetonitrile (MeCN), methanol (MeOH) and water (H_2O) resulted in the growing of completely inorganic single crystals of $CsPbBr_3$. The saturated solution of $MeCN$ and $MeOH$ is yellow-orange color, while that of H_2O showed white colored precipitates due to its bleaching capability. Filtration allows the removal of the impurities from the precipitates of$MeCN$ and $MeOH$ saturated solution. Orange hue crystals vanish after heating the crystal combination to a target temperature of 50°C for 24 hours till it turns yellow-green and orange. This is followed by cooling the solution to room temperature while stirring constantly. Again, filtration might be used to further remove undesirable crystals from the cooled solution. The desired crystals of CsPbBr3 can be obtained by slowly heating this solution to a temperature over 120°C for MeCN and 40°C for Me OH. Saidaminov et.al. [62] Grew single crystals of $CsPbBr_3$ using MITC method by varying the precursor's molar ratio. Two precursors $CsBr$ and $PbBr_2$ were taken in the molar ratio 1:2 followed by the filtration of the solution at temperature 100°C. The filtered solution was heated again at a temperature of 120°C for 3hr to obtain pure shape controlled crystal of $CsPbBr_3$. In case of a molar ratio of 1:1 and 1:1.5 for CsBr and $PbBr_2$ results in the formation of undesired crystals of Cs_4PbBr_6 at temperature 120°C. The fundamental properties of the synthesized crystal such as photoluminescence and optical absorption were also explored [26].

VI. CONCLUSION AND FUTURE OUTLOOK

In this chapter, a basic idea about perovskite structure having general formula ABX_3 is discussed in brief along with the properties of some perovskite crystal materials. Tolerance factor (*t*) is one of the parameters that can predict the formation of ideal perovskite structures. A value of *t* ranging between 0.9-1.0 would result in perovskite formation. Different solvents such as GBL, DMF, DMSO, and NMP are suitable for better solubility to various precursors. GBL is an appropriate solvent for I-based perovskites, whereas the DMF is an appropriate for Br-based perovskite. A comprehensive elucidation of three growing methods based on the ease of methodology and cost effectiveness, for perovskite single crystals and its investigation of various properties namely carrier mobility, carrier diffusion length, carrier life time, and trap density values that directly affects the optoelectronic application is presented. ITC method provides a faster growth rate of perovskite crystals as compared to others. Perovskite single crystals provide favourable material choice for fabrication of high performance solar cells and photodetectors. Many works are restricted to grow only large size crystals, but there are several factors that need to be understood, for the stability and toxicity of large scale production. In comparison to polycrystallines, thin-film halide based single crystal perovskites have been shown to be a far better possibility for optoelectronic applications. In several studies researchers have focused on the analysis of hybrid perovskites's crystal quality; however some of its properties such as grain boundaries, defects, trap density, and their interconnection is equivocal. Hence, to understand the basic characteristics and physics of hybrid perovskites, need to grow high quality single crystal of hybrid perovskite, more rumination should be required to their growth process and defects. The device based on a single crystal perovskite with varying dimensions would also be a key research topic, and it is imperative to look for several new applications.

VII. ACKNOWLEDGEMENTS

The author is grateful to the university grant commission (UGC) for providing financial support to carry out this work.

REFERENCES

[1] S.K. Sahoo, B. Manoharan, N. Sivakumar, Introduction: Why perovskite and perovskite solar cells? Elsevier Inc., 2018. https://doi.org/10.1016/B978-0-12-812915-9.00001-0.
[2] W.S. Yang Iodide management in formamidinium-lead-halide-based perovskite layers for efficient solar cells. Science **356**, 1376-1379 (2017).
[3] N.J. Jeon et.al. Solvent engineering for high-performance inorganic-organic hybrid perovskite solar cells. Nat. Mater. **13**, 897-903 (2014).
[4] M. Abdi-JalebiMaximizing and stabilizing luminescence from halide perovskites with potassium passivation. Nat.**555**, 497-501 (2018).
[5] Y. Wang Stabilizingheterostructures of soft perovskite semiconductors. Science **365**, 687-691 (2019).
[6] J.J. Yoo An interface stabilized perovskite solar cell with high stabilized efficiency and low voltage loss. Energy Environ. Sci. **12**, 2192-2199 (2019).
[7] H. Min Efficient, stable solar cells by using inherent bandgap of α-phase formamidinium lead iodide. Science **366**, 749-753 (2019).
[8] Kojima, K. Teshima, Y. Shirai, T. Miyasaka, Organometal Halide Perovskites as Visible-Light Sensitizers for Photovoltaic, J. Am. Chem. Soc. 6050–6051(2009). https://doi.org/10.1021/ja809598r.
[9] M.Powalla, S. Paetel, E. Ahlswede, R. Wuerz, C. D. Wessendorf,T.M. Friedlmeier,
[10] Thin film solar cells exceeding 22% solar cell efficiency: An overview on CdTe-,
[11] Cu(In,Ga)Se2-, and perovskite-based materials, Appl. Phy. Rev. **5,** (2018)
[12] 041602; https://doi.org/10.1063/1.5061809.
[13] M.A. Green, Y. Hishikawa, E.D. Dunlop, D.H. Levi, J.H.-Ebinger, M. Yoshita, A.Y.W. Ho-Baillie, Solar cell efficiency tables (Version 53), Progress in Photovoltaics: Research and Applications **27**(1) (2018).
[14] J. J. Yoo Efficient perovskite solar cells via improved carrier management. Nature **590**, 587-593 (2021).
[15] J.F. Guillemoles Guide for the perplexed to the Shockley-Queisser model for solar cells. Nat. Photon. **13**, 501-505 (2019).
[16] Website: https://www.nrel.gov/pv/cell-efficiency.html
[17] H. Zheng, J. Duan, J. Dai, Synthesis of formamidinium lead iodide perovskite bulk single crystal and its optical properties, Int. J. Mod.Phys. B. **31,** 1–5(2017).https://doi.org/10.1142/S0217979217440660.
[18] M.I. Saidaminov, A.L. Abdelhady, G. Maculan, O.M. Bakr, Retrograde solubility of formamidinium and methylammonium lead halide perovskites enabling rapid single crystal growth, Chem. Commun. **51**, 17658–17661(2015).https://doi.org/10.1039/c5cc06916e.
[19] F.F. Targhi, Y.S. Jalili, F. Kanjouri, MAPbI3 and FAPbI3 perovskites as solar cells: Case study on structural, electrical and optical properties, Results Phys. **10**, 616–627(2018). https://doi.org/10.1016/j.rinp.2018.07.007.
[20] Z. Yi, H. Ladi, X. Shai, H. Li, Y. Shen, M. Wang, Will organic – inorganic hybrid halide lead perovskites be eliminated from optoelectronic applications?, Nanoscale Advances 1276–1289(2019). https://doi.org/10.1039/c8na00416a.
[21] Q. Han, S.H. Bae, P. Sun, Y.T. Hsieh, Y. Yang, Y.S. Rim, H. Zhao, Q. Chen, W. Shi, G. Li, Y. Yeng, Single Crystal Formamidinium Lead Iodide (FAPbI3): Insight into the Structural, Optical, and Electrical Properties, Adv. Mater. **28,** 2253–2258(2016).https://doi.org/10.1002/adma.201505002.
[22] M. Wright, A. Uddin, Organic-inorganic hybrid solar cells: A comparative review, Sol. Energy Mater. Sol. Cells.**107**, 87–111(2012).https://doi.org/10.1016/j.solmat.2012.07.006.
[23] S. Günes, N.S. Sariciftci, Hybrid solar cells, InorganicaChim. Acta.**361**, 581–588 (2008).https://doi.org/10.1016/j.ica.2007.06.042.
[24] Semiconductor devices, Physics and technology, Second edition by S. M. Sze.
[25] S. Lv, S. Pang, Y.Zhou, N. Padure, H.Hu, W. Li, X. Zhou, H. Zhu, L. Zhang, C.Huang, G. Cui, A. Manuscript,One-step solution-processed formamidinium lead trihalide ($FAPbI_{(3-x)}Cl_x$) for mesoscopicperovskitepolymer solar cells. (2013)
[26] www.rsc.org/pccp, (n.d.). https://doi.org/10.1039/x0xx00000x.

[27] R. Babu, L. Giribabu, S.P. Singh, Recent Advances in Halide-Based Perovskite Crystals and Their Optoelectronic Applications, Crystal growth Design **18**, 2645-64(2018). https://doi.org/10.1021/acs.cgd.7b01767.

[28] G.E. Eperon, S.D. Stranks, C. Menelaou, M.B. Johnston, L.M. Herz, H.J. Snaith, Formamidinium lead trihalide: A broadly tunableperovskite for efficient planar heterojunction solar cells, Energy Environ. Sci. **7**, 982–988(2014).https://doi.org/10.1039/c3ee43822h.

[29] Z. Li, M. Yang, J. Park, S. Wei, J.J. Berry, K. Zhu, Stabilizing Perovskite Structures by Tuning Tolerance Factor: Formation of Formamidinium and Cesium Lead Iodide Solid-State Alloys, Chemistry of Materials **2**, 284-92 (2016). https://doi.org/10.1021/acs.chemmater.5b04107.

[30] S. Arya, P. Mahajan, R. Gupta, R. Srivastava, V. Gupta, A comprehensive review on synthesis and applications of single crystal perovskite halides, Prog. Solid State Chem. 100286(2020).https://doi.org/10.1016/j.progsolidstchem.2020.100286.

[31] C.J. Bartel, C. Sutton, B.R. Goldsmith, R. Ouyang, C.B. Musgrave, L.M. Ghiringhelli, M. Scheffler, New tolerance factor to predict the stability of perovskite oxides and halides, Sci. Adv. 1–10(2019).

[32] Z. Arain, C. Liu, Y. Yang, M. Mateen, Y. Ren, Y. Ding, X. Liu, Elucidating the dynamics of solvent engineering for perovskite solar cells, Sci China Mater. 161-172(2019).https://doi.org/10.1007/s40843-018-9336-1.

[33] M. Abd, F. Aziz, A. Fauzi, W. Norharyati, W. Salleh, N. Yusof, J. Jaafar, T. Soga, M. Zainizan, N. Ahmad, Towards high performance perovskite solar cells : A review of morphological control and HTM development, Appl. Mater. Today.**13**, 69–82(2018).https://doi.org/10.1016/j.apmt.2018.08.006.

[34] M.I. Saidaminov, A.L. Abdelhady, B. Murali, E. Alarousu, V.M. Burlakov, W. Peng, I. Dursun, L. Wang, Y. He, G. Maculan, A. Goriely, T. Wu, O.F. Mohammed, O.M. Bakr, High-quality bulk hybrid perovskite single crystals within minutes by inverse temperature crystallization, Nat. Commun. 1–6(2015).https://doi.org/10.1038/ncomms8586.

[35] C.C. Stoumpos, C.D. Malliakas, J.A. Peters, Z. Liu, M. Sebastian, J. Im, T.C. Chasapis, A.C. Wibowo, D.Y. Chung, A.J. Freeman, B.W. Wessels, M.G. Kanatzidis, Crystal Growth of the Perovskite Semiconductor CsPbBr 3 : A New Material for High-Energy Radiation Detection, **13**, 2722-2727 (2013).http://doi.org/10.1021/cg400645t

[36] M. Rodová, J. Bro, K. Kní, K. Nitsch, Phase Transitions In Ternary Caesium Lead Bromide, **71**, 667–673(2003).

[37] P. Zhang, G. Zhang, L. Liu, D. Ju, L. Zhang, K. Cheng, X. Tao, Anisotropic Optoelectronic Properties of Melt-Grown Bulk CsPbBr3 Single Crystal, J. Phys. Chem. Lett. **9**, 5040–5046(2018).https://doi.org/10.1021/acs.jpclett.8b01945.

[38] T. Ye, W. Fu, J. Wu, Z. Yu, X. Jin, H. Z. chen, H. Li, Single-Crystalline Lead Halide Perovskite Arrays for Solar Cells, A. Manuscript, Materials Chemistry A, (2015). https://doi.org/10.1039/C5TA10155G.

[39] T. Zhang, M. Yang, E.E. Benson, Z. Li, J. Van De Lagemaat, J.M. Luther, Y.Yan, K. Zhu, Y. Zhao, A Facile Solvo-Thermal Growth of Single Crystal Mixed HalidePerovskite$CH_3NH_3Pb(Br_{1-x}Cl_x)_3$ C. Commun, ChemComm, (n.d.). https://doi.org/10.1039/b000000x.

[40] Y. Fang, Q. Dong, Y. Shao, Y. Yuan, J. Huang, Highly narrowband perovskite single-crystal photodetectors enabled by surface-charge recombination, (2015). https://doi.org/10.1038/nphoton.2015.156.

[41] Y. Dang, Y. Liu, Y.Sun, D. Yuan, X. Liu, W. Lu, G. Liu, H. Xia, X. Tao, Bulk crystal growth of hybrid perovskite material $CH_3NH_3PbI_3$, CrystEngComm. 1–6(2014).https://doi.org/10.1039/C4CE02106A.

[42] Q. Dong, Y. Fang, Y. Shao, J. Qiu, L. Cao, J. Huang, Electron-hole diffusion lengths > 175 μm in solution-grown $CH_3NH_3PbI_3$ single, 1–8 (2015).http://doi.org/10.1126/science.aaa5760.

[43] D. Shi, V. Adinolfi, R. Comin, M. Yuan, E. Alarousu, A. Buin, Y. Chen, S. Hoogland, A. Rothenberger, K. Katsiev, Y. Losovyj, X. Zhang, P.A. Dowben, O.F. Mohammed, E.H. Sargent, O.M. Bakr, Low trap-state density and long carrier diffusion in organoleadtrihalide perovskite single crystals, **347** 519–522(2015).

[44] F. Liu, F. Wang, K.R. Hansen, X. Zhu, Bimodal Bandgaps in Mixed CesiumMethylammonium Lead Bromide Perovskite Single Crystals, J. Phys. Chem. C. **123,** 14865–14870(2019). https://doi.org/10.1021/acs.jpcc.9b03536.

[45] H. Wei, Y. Fang, P. Mulligan, W. Chuirazzi, H. Fang, C. Wang, B.R. Ecker, Y. Gao, M.A. Loi, L. Cao, Sensitive X-ray detectors made of methylammonium lead tribromideperovskite single crystals, Nat. Photonics. 1–8(2016).https://doi.org/10.1038/nphoton.2016.41.

[46] D.B. Mitzi, A Layered Solution Crystal Growth Technique and the Crystal Structure of $(C_6H_5C_2H_4NH_3)_2PbCl_4$, **704**, 694–704(1999).

[47] W. Liao, Y. Zhang, C. Hu, J. Mao, H. Ye, P. Li, S. D. Huang and R. G. Xiong, A lead-halide perovskite molecular ferroelectric semiconductor, Nat. Commun.1–7(2015).https://doi.org/10.1038/ncomms8338.
[48] M. Daub, H. Hillebrecht, Synthesis, Single-Crystal Structure and Characterization of $(CH_3NH_3)_2Pb(SCN)_2I_2$, 11016–11017(2015). https://doi.org/10.1002/anie.201506449.
[49] Y. Dang, D. Ju, L. Wang, X. Tao, Recent Progress in the Synthesis of Hybrid Halide Perovskite Single Crystals, Cryst. Engg.Comm. (2016).https://doi.org/10.1039/C6CE00655H.
[50] J. Ding, Q. Yan, Progress in organic-inorganic hybrid halide perovskite single crystal: growt techniques and applications, Sci China Materials **60**, 1063–1078 (2017).https://doi.org/10.1007/s40843-017-9039-8.
[51] G. Maculan, A.D. Sheikh, A.L. Abdelhady, M.I. Saidaminov, A. Haque, B. Murali, E. Alarousu, O.F. Mohammed, T. Wu, O.M. Bakr, $CH_3NH_3PbCl_3$ Single Crystals: Inverse Temperature Crystallization and Visible-Blind UV-Photodetector, Phy. Chem. Lett. 6–11(2015).https://doi.org/10.1021/acs.jpclett.5b01666.
[52] J.M. Kadro, K. Nonomura, D. Gachet, M. Grätzel, A. Hagfeldt, Facile route to freestanding $CH_3NH_3PbI_3$ crystals using inverse solubility, Nat. Publ. Gr. 1–6(2015). https://doi.org/10.1038/srep11654.
[53] D.N. Dirin, I. Cherniukh, S. Yakunin, Y. Shynkarenko, M. V Kovalenko, Solution-Grown $CsPbBr_3$Perovskite Single Crystals for Photon Detection, Chem. Mater.8470-74(2016).https://doi.org/10.1021/acs.chemmater.6b04298.
[54] S. Kawachi, M. Atsumi, N. Saito, N. Ohashi, Y. Murakami, J. Yamaura, Structural and Thermal Properties in Formamidinium and Cs-Mixed Lead Halides, 6967-72(2019). https://doi.org/10.1021/acs.jpclett.9b02750.
[55] L. Chen, Y. Tan, Z. Chen, T. Wang, S. Hu, Z. Nan, L. Xie, Y. Hui, J. Huang, C. Zhan, S. Wang, J. Zhou, J. Yan, B. Mao, Toward Long-Term Stability: Single-Crystal Alloys of Cesium-Containing Mixed Cation and Mixed Halide Perovskite, J. Am. Chem. Soc. **141**, 1665–1671(2019). https://doi.org/10.1021/jacs.8b11610.
[56] M. Pratheek, P. Predeep, Hybrid perovskite single crystal with extended absorption edge and environmental stability : Towards a simple and easy synthesis procedure, Mater. Chem. Phys. **239**, 122084(2020).https://doi.org/10.1016/j.matchemphys.2019.122084.
[57] Y. Liu, Y. Zhang, X. Zhu, J. Feng, I. Spanopoulos, W. Ke, Y. He, X. Ren, Z. Yang, F. Xiao, K. Zhao, M. Kanatzidis, S. Liu, Triple-Cation and Mixed-Halide Perovskite Single Crystal for High Performance X-ray Imaging, Adv. Material (2021). https://doi.org/10.1002/adma.202006010.
[58] Y. Liu, J. Sun, Z. Yang, D. Yang, X. Ren, H. Xu, Z. Yang, S.F. Liu, 20-mm-Large Single-Crystalline Formamidinium-Perovskite Wafer for Mass Production of Integrated Photodetectors, Adv. Opt. Mater. **4**, 1829–1837(2016).https://doi.org/10.1002/adom.201600327.
[59] Y. Liu, Z. Yang, D. Cui, X. Ren, J. Sun, X. Liu, J. Zhang, Q. Wei, H. Fan, F. Yu, X. Zhang, Two-Inch-Sized Perovskite $CH_3NH_3PbX_3$ (X = Cl , Br , I) Crystals : Growth and Characterization, Adv. Mater. **3**, 5176–5183(2015).https://doi.org/10.1002/adma.201502597.
[60] D. Yang, C. Xie, J. Sun, H. Zhu, X. Xu, P. You, S.P. Lau, Amplified Spontaneous Emission from Organic – Inorganic Hybrid Lead Iodide Perovskite Single Crystals under Direct Multiphoton Excitation, Adv. Optical Mater. 1053–1059(2016).https://doi.org/10.1002/adom.201600047.
[61] M. Sheik-bahae, A.L.I.A. Said, T. Wei, Sensitive Measurement of Optical Nonlinearities Using a Single Beam, IEEE Journal of Quantum Electronics 760-9(1990).
[62] G. Walters,B. Sutherland, S. Hoogland, D. Shi, Riccardo Comin, D. Sellan, M. Bakr,
[63] Edward. H. Sargent, Two-Photon Absorption in Organometallic Bromide Perovskites,
[64] Acs Nano 9340-6(2015).
[65] R.S. Santosh, S.V. Rao, L. Giribabu, D.N. Rao, Femtosecond and nanosecond nonlinear optical properties of alkyl phthalocyanines studied using Z-scan technique, Chemial Physical Letters **447**, 274–278(2007). https://doi.org/10.1016/j.cplett.2007.09.028.
[66] H. S. Rao, B. Chen, X. Wang, D. Kuang, C. Y. Su Micron-scale Laminar $MAPbBr_3$ Single Crystal for Efficient and Stable Perovskite Solar Cell A. Manuscript, ChemComm, (2017).https://doi.org/10.1039/C7CC02447A.
[67] Y. Rakita, N. Kedem, S. Gupta, A. Sadhanala, V. Kalchenko, M.L. Bo, M. Kulbak, R.H. Friend, D. Cahen, G. Hodes, Low-Temperature Solution-Grown $CsPbBr_3$ Single Crystals and Their Characterization, Amer. Chem. Soc. 5717−5725(2016). https://doi.org/10.1021/acs.cgd.6b00764.
[68] M.I. Saidaminov, A. Haque, J. Almutlaq, S. Sarmah, X. Miao, R. Begum, A.A. Zhumekenov, I. Dursun, N. Cho, B. Murali, O.F. Mohammed, T. Wu, O.M. Bakr, Inorganic Lead Halide Perovskite Single Crystals : Phase-Selective Low-Temperature Growth , Carrier Transport Properties , and Self-Powered Photodetection, Adv. Optical Mater.1600704(2017).https://doi.org/10.1002/adom.201600704.

